J Ind Microbiol Biotechnol (2011) 38:113–125
DOI 10.1007/s10295-010-0836-0

ORIGINAL PAPER

# Xylanase II from *Trichoderma reesei* QM 9414: conformational and catalytic stability to Chaotropes, Trifluoroethanol, and pH changes

**G. López · A. Bañares-Hidalgo · P. Estrada**

Received: 25 March 2010 / Accepted: 26 July 2010 / Published online: 14 September 2010


**Abstract** Xylanase II, a key enzyme in the hydrolysis of xylan, was purified from cultures of *Trichoderma reesei* QM 9414 (anamorph of *Hypocrea jecorina*) grown on wheat straw as a carbon source. Xylanase treated with increasing guanidinium hydrochloride concentrations was denatured in a cooperative way regarding secondary and tertiary structures with midpoint transitions 5.6 ± 0.1 and 3.7 ± 0.1 M, respectively, whereas the enzymatic activity showed an intermediate state at 2–4 M denaturant. Treatment with urea showed that xylanase secondary structure was stabilized up to 4 M urea to be destabilized thereafter in a cooperative way with a transition midpoint Dm = 5.7 ± 0.2 M, but the ellipticity at 220 nm was greater than control in the presence of urea up to 6 M. Tertiary structure in the presence of urea showed also intermediate states with partial cooperative transitions with a midpoint: Dm = 2.7 ± 0.04 and 6.7 ± 0.3 M, respectively, whereas the enzymatic activity was enhanced about 40% at 2 M and inhibited above 4 M urea. Assays with the fluorescent probe 4,4′-bis-1-phenylamine-8-naphftalene sulfonate (bis-ANS) proved that the intermediate states had the characteristics of molten globule structures. The change of free energy for xylanase in absence of denaturants obtained from the spectral centre of mass (SCM) data at 298 K is $\Delta G^0_{H_2O} = \sim 17$ kJ mol$^{-1}$. In the presence of increasing trifluoroethanol (TFE), the enzyme gained α-helix content and lose tertiary structure and catalytic activity. Changes in pH (2–9) had practically no effect on the secondary structure of the enzyme, whereas the SCM values indicated that tertiary structure is maintained above pH 4. Bis-ANS binds to xylanase at pH 2 and 2.5 and in the presence of 30–40% TFE (v/v) characterizing molten globule states in those environmental conditions.

**Keywords** Xylanase II · *Trichoderma reesei* · Stability · Urea · Guanidinium hydrochloride · Trifluoroethanol · pH

## Introduction

Xylan is the major hemicellulose component in plant cell walls and the most abundant polysaccharide after cellulose [3]. The filamentous fungus *Trichoderma reesei* produces extracellular enzymes that degrade xylan into monomers. The major components of this xylanolytic system are xylanase (β-1,4-D-xylan xylanohydrolase; EC 3.2.1.8) which hydrolyses the β-1,4 bonds in the main chain generating a mixture of xylo-oligosaccharides and β-xylosidase (β-1,4-D-xylan xylohydrolase; EC 3.2.1.37), which cleaves off the terminal xylose units from the non-reducing end of xylo-oligosaccharides and is rate-limiting in xylan hydrolysis [37]. To date, four xylanases have been described in *Trichoderma reesei*: xylanase I (XYN I, 19 kDa, pI ~ 5.2), XYN II, one of the major xylanases of the fungus (21 kDa, pI ~ 9) [42, 43], XYN III (32 kDa, pI ~ 9.1) practically absent in *T. reesei* QM 9414 [49] and XYN IV (50.3 kDa, pI ~ 7) [32].

The industrial use of xylanases is well known and is extended to several fields. First, xylanases are used in the prebleaching of kraft pulp by improving the liberation of lignin through hydrolysis of hemicellulose. Therefore, they reduce the use of harsh chemicals in the subsequent

This article is part of the BioMicroWorld 2009 Special Issue.

G. López · A. Bañares-Hidalgo · P. Estrada (✉)
Departamento de Bioquímica y Biología Molecular I.,
Facultad de Biología, Universidad Complutense,
28040 Madrid, Spain
e-mail: estrada@bbm1.ucm.es

chemical bleaching stages [47]. In the textile industry, xylanases are an alternative to the sulfuric acid treatment of the textile polyester-cellulose wastes [5]. In the food industry, xylanases improve dough properties and baking quality of baked goods by breaking down the polysaccharides in the dough [25]. The easy cultivation of the fungus *Trichoderma reesei* according to the high activity of some of its xylanases, makes it very attractive from an industrial point of view. According to the biotechnological importance of xylanases, thermoinactivation studies and improvement of their thermostability has attracted a considerable amount of work with different techniques [2, 6, 19, 45], whereas structure–function studies of these enzymes are limited. Enzymes must have flexible active sites that undergo rapid conformational transitions to catalyze sequential chemical transformations to accommodate different chemical intermediates. One approach to investigate the role of active site flexibility in enzyme catalysis is to determine the effects of chaotropic agents, such as urea and guanidinium hydrochloride (GdmCl), which may stabilize alternative conformational states. Regarding xylanases, circular dichroism, fluorescence emission and enzymatic assays are the common techniques employed to detect intermediate states. The GdmCl-induced unfolding of XynA from *Thermotoga maritime* showed intermediate states [48] and so did xylanase from *Pseudoalteromonas haloplanktis* [7], whereas xylanase A from *Streptomyces lividans* exhibited a biphasic transition in the unfolding process with GdmCl [36]. Moreover, the refolding of an intermediate state obtained with 2 M GdmCl of xylanase from *Penicillium citrinum* was carried out with the chaperone α-crystallin [10], and xylanase from the thermophilic *Bacillus* sp. unfolded in the presence of 6 M GdmCl or 8 M urea has been refolded through the assistance of cyclodextrins whereas an intermediate state was detected at very low GdmCl concentration [28]. Also, many enzymes are either activated or inactivated by urea or GdmCl concentrations that are lower than those needed to cause demonstrable structural changes [12] as is shown with xylanase activity from *Chainia*, which is stimulated at low urea concentrations while subtle changes were noted in the secondary and tertiary structure of the enzyme [22]. In addition, the aggregation and ulterior solubilization of xylanase from *Clostridium stercorarium* has been studied [13], whereas 0.25 M GdmCl was a competitive inhibitor for xylanase from an alkalophilic thermophilic *Bacillus* sp. [29]. GdmCl and/or urea have also been employed to achieve the reversibility of calorimetric transitions in xylanase from *Bacillus* circulans [8] or to asses the stability of xylanase mutants of *Streptomyces olivaceoviridis* [21].

Over the past years, we have studied the production of cellulolytic enzymes by the fungus *T. reesei* QM 9414 grown on wheat straw [1] as well as the purification and kinetic characterization of $\beta$-glucosidase [11]. Regarding hemicellulases, we have purified [26] and studied the kinetic and chemical mechanism of $\beta$-xylosidase [15, 16], immobilized it on nylon powder, and studied its stability to temperature on a bioreactor [9]. We have also purified xylanase II and studied the protective role of several polyols on its thermoinactivation [6]. The present paper focuses on the field of enzyme structure–function relations by studying the stability of xylanase II to several agents such as chaotropes (urea and guanidinium hydrochloride), alcohols (2,2,2-trifluoroethanol), and pH. Structural stability was investigated by means of circular dichroism and fluorescence spectroscopy and results were correlated with the catalytic activity of the enzyme.

## Materials and methods

### Enzyme purification

*Trichoderma reesei* QM 9414 was cultured on wheat straw as previously described [1]. Xylanase was purified from culture supernatant following the same procedure described for $\beta$-glucosidase purification [11, 26] including ammonium sulphate precipitation, DEAE-Sepharose CL-6B (Pharmacia, Uppsala, Sweden) and Ultrogel AcA 44 (LKB, Uppsala, Sweden) cromatographies. Purification of xylanase to homogeneity was achieved after the gel filtration step and the fractions corresponding to the top of the elution peak were pooled and employed for structural stability studies. The purity of xylanase was routinely checked by SDS-PAGE and amino acid analysis.

### Analytics

Amino acid analysis of xylanase (0.8–2.3 nmol) was determined on a Biochrom 30 automatic amino acid analyzer after hydrolysis with 6 N HCl at 105°C for 24 h in sealed tubes under vacuum. The protein concentration of samples was calculated from their absorbance at 280 nm using the experimental molar absorption coefficient $\varepsilon_{280} = 58{,}453 \pm 212\ M^{-1}\ cm^{-1}$, calculated from the amino acid content, which is very similar to the theoretical one ($58{,}330\ M^{-1}\ cm^{-1}$) at the same wavelength [18]. When the protein content was measured according to Lowry et al. [24] with bovine serum albumin (BSA, Sigma) as standard, the concentration of xylanase II was overestimated, perhaps due to its high number of tyrosine residues. Reducing sugars were measured by the dinitrosalicylic reagent method [27] recording the absorbance of the reduced reagent at 640 nm in a Beckman DU-800 spectrophotometer with D-xylose (Sigma) as standard.

### Enzymatic assays

Standard assays were carried out in centrifuge tubes with 2 ml of 100 mM sodium citrate buffer pH 5 (standard buffer) containing 1.4 μg protein and 1% (w/v) beechwood xylan (Sigma) at 55°C for 10 min in a water bath (Selecta). The reaction was terminated by cooling the samples in ice for 10 min and the samples were centrifuged at 3,000 rpm in a desk centrifuge for 10 min. To 1 ml of the supernatant, 1.5 ml of 3,5-dinitrosalycilic acid (DNS, Sigma) was added and the samples were boiled for 5 min, cooled in water–ice, and analyzed for reducing sugars. All the experiments were carried out in duplicate or triplicate and non-enzymatic hydrolysis of xylan was subtracted in each experiment.

### Circular dichroism studies

Circular dichroism spectra of xylanase were recorded at 25°C on a Jasco J-715 spectropolarimeter in thermostated quartz cells of 0.1-cm path length, at 50 nm $min^{-1}$ (1 s response time) for the far-UV (240–200 nm) spectral range, each spectrum being the accumulation of five scans. The spectra were obtained with 0.09 mg $ml^{-1}$ protein in 250 μl of 20 mM citrate buffer pH 5. Molar ellipticity $[\theta]$ was obtained from raw ellipticity data, $\theta$, according to: $[\theta] = \theta/(10clN)$ where l is the path-length cell, $c$ the concentration (M), and $n$ is the number of amino acids (190). The molecular mass of xylanase II was the theoretical one (20,842 Da) according to DNA Star program (DNAstar Inc., MD, USA). Estimations of the secondary structure content from the CD spectra were performed by using the CDPro program and the α-helix and $\beta$-sheet contents were calculated using three different methods, CONTIN/LL, SELCON3, and CDSSTR [39] employing their mean value in plots. When spectra were recorded in the presence of urea (Sigma), guanidium hydrochloride (Sigma) and trifluoroethanol (Merck), the protein was previously preincubated with them for ~1 h at 25°C. Samples of 219 μl were prepared in water at the corresponding chaotrope concentration from stock solutions of 9.87 M urea and 9.75 M GdmCl in water. We added to them 31 μl protein from a stock solution (0.725 mg $ml^{-1}$) in 100 mM citrate buffer pH 5 so that the final 250 μl preincubation mixture contained 0.09 mg $ml^{-1}$ protein in 12.4 mM citrate buffer pH 5 (citrate molarity for CD studies must not surpass 20 mM because of the background of the buffer signal). Samples preincubated with TFE were prepared by adding 31 μl protein of the same stock to 219 μl of TFE mixtures prepared by diluting commercial TFE with the appropriate water amount to reach the desired final percent TFE (v/v). To record the CD variation with pH, the spectra were obtained of 250 μl samples of 5 mM citrate, 5 mM MES, and 5 mM Tris buffer (CMT buffer) at the indicated pHs containing 0.1 mg $ml^{-1}$ of purified xylanase. The pH was assessed in a Mettler-Toledo MP230 pH-meter provided with a microelectrode. Spectra from control samples were protein was substituted by the corresponding buffer were subtracted routine to spectra obtained in the presence of protein.

### Intrinsic and extrinsic fluorescence spectroscopy studies

The intrinsic fluorescence emission spectra of xylanase were recorded at 20°C in a SLM-Aminco AB2 spectrofluorimeter using a 1-cm quartz cell with 290-nm excitation and emission slits set at 4 nm and scan speed of 2 nm $s^{-1}$. The sample contained 0.09 mg $ml^{-1}$ in 250 μl of 20 mM citrate buffer pH 5. When spectra were recorded in the presence of urea, GdmCl and TFE, xylanase was preincubated with them for ~4 h at 25°C. Samples containing TFE, the chaotropes and samples at different pHs were prepared as described above for obtaining the CD spectra. Spectra from control samples where protein was substituted by the corresponding buffer were subtracted routine to spectra obtained in the presence of protein.

Extrinsic fluorescence of bis-ANS probe (4,4′-bis-1-phenylamine-8-naphtalene sulfonate from Molecular Probes) was determined as follows. Samples were prepared in a final volume of 200 μl by adding 7 μl of probe from a 0.23-mM solution in methanol to 18 μg protein in CMT buffer at the corresponding pH (final probe concentration 8 μM). After incubation at 37°C for 5 min, the emission spectra (400–625 nm) were recorded after excitation at 395 nm in the spectrofluorimeter connected to a water-bath thermostatized at 37°C. Samples without protein were the blank. Scan speed and slit widths were as described above. The same protocol was applied to samples containing GdmCl, urea or 2,2,2-trifluoroethanol (TFE) except that pH 5 was employed.

### Analysis of the data

The SCM, intensity-weighted average emission wavelength, was calculated from fluorescence spectra according to the following equation where $\lambda$ is the emission wavelength and $I(\lambda)$ represents the fluorescence intensity at wavelength $\lambda$.

$$SCM = \Sigma\lambda I(\lambda)/\Sigma I(\lambda) \quad (1)$$

The fitting of the experimental data from denaturation experiments was according to the following equations.

$$Y_{obs} = Y_N + a/(1 + \exp(-(D - Dm)/b)) \quad (2)$$

$$\Delta G^0 = -RT \ln(Y_N - Y_{obs})/(Y_{obs} - Y_U) \quad (3)$$

$$\Delta G^0 = \Delta G^0_{H_2O} - mD \quad (4)$$

In Eqs. (2), (3), and (4), $Y_{obs}$ is the observed parameter (SCM or $[\theta]^{220}$) at each denaturant concentration, $Y_N$ and $Y_U$ are the parameter values in native and unfolded conditions, respectively, $D$ is the denaturant concentration, Dm is the denaturant concentration at which half of the protein is unfolded (the midpoint transition), $a$ and $b$ are constants, $\Delta G^0$ is the change of free energy (kJ mol$^{-1}$) at a given denaturant concentration, $\Delta G^0_{H_2O}$ is the change of free energy in water, m is the slope of the line (kJ mol$^{-1}$ M$^{-1}$) $R$ the gas constant (8.314 J mol$^{-1}$ K$^{-1}$) and $T$ the absolute temperature (K).

## Results

Studies on xylanase stability were carried out in the presence of GdmCl, urea, trifluoroethanol and pH ranging from 2 to 9. Far-UV circular dichroism (CD) and fluorescence intensity spectra of the samples were recorded at 25°C. Also, enzymatic assays were carried out, unless otherwise stated, after preincubating the enzyme with the reagent or with the buffer at the indicated pH.

### Unfolding of xylanase by guanidinium hydrochloride

The unfolding of xylanase induced by increasing concentrations of GmdCl (0–8.5 M) monitored by far-UV CD, intrinsic fluorescence spectroscopy, and enzymatic assays are depicted in Fig. 1. The protein was preincubated with the denaturant for 1 h at 25°C and the CD spectra were recorded at 25°C. Figure 1a depicts the xylanase spectra without denaturant and in the presence of 8.5 M GdmCl. In the control sample, the following percent content of secondary structure were calculated: 19.6 ± 0.8% α-helix, 40.9 ± 3.5% $\beta$-sheet, 19.5 ± 1.2% turn, and 19.5 ± 3.4% random. At the highest GdmCl concentration, the shape of the spectrum indicates that the protein is unfolded. Figure 1b shows the variation of the molar ellipticity at 220 nm ($[\theta]^{220}$) with increasing GdmCl concentrations. Above ~4.5 M denaturant, $[\theta]^{220}$ increases cooperatively, which indicates that there are only two states with no accumulation of stable intermediates, regarding the secondary structure of xylanase, and one of them is the unfolded one. Experimental data above 2.5 M were fitted to Eq. (2) obtaining a midpoint transition Dm = 5.6 ± 0.1 M, Dm being the denaturant concentration at which half of the protein is unfolded, regarding the backbone conformation. Data mentioned above are summarized in Table 1.

The fluorescence spectra of the enzyme with and without GdmCl were also recorded at 25°C. The fluorescence intensity was increased with denaturant concentration and the maximum wavelength above 3 M GdmCl was also increased (not shown). Figure 1c represents the variation of the spectral center of mass (SCM, the intensity-weighted average emission wavelength) as the denaturant concentration is increased. The SCM is taken to represent the variation in the whole spectrum of the protein and we see that there is a cooperative transition in Fig. 1c, indicating that the tertiary structure of the enzyme also unfolds in a two-state process. The fitting of the data to Eq. (2) gave a midpoint transition Dm = 3.7 ± 0.1 M, which is smaller than the obtained by processing the $[\theta]^{220}$ data. This indicates that the protein tertiary structure is lost at lower GdmCl concentration than the secondary one. Moreover, the fact that both curves (SCM and $[\theta]^{220}$) do not coincide points to the existence of an intermediate state, thereby the xylanase unfolding by GdmCl is not a two-state process. The following step was to parallel the conformational studies described above with the enzymatic behavior of xylanase under the effect of GdmCl. To this, the enzymatic stability of xylanase was determined in the beechwood xylan degradation. In order to get stable intermediate states, we approached the experiment by preincubating the enzyme with the denaturant instead of carrying out the enzymatic assay in the presence of the denaturant as is usually done. To this, the enzyme was preincubated in 100 µl of standard buffer with 0–7.2 M denaturant for 24 h at 4°C and then the sample was diluted 20 times with the standard buffer and the substrate to a final reaction volume of 2 ml. Thus, the actual denaturant concentration in the enzymatic assay was very low, in the range 0–0.36 M. Figure 1d shows the residual activity of xylanase as the GdmCl concentration (in the preincubation) was increased. We see a gradual decrease in activity, then a plateau with residual activity around 75%, and a cooperative transition with Dm = 4.9 ± 0.05 M thereafter. These results point to the existence of an intermediate state of xylanase at ~2–4 M GdmCl with reduced activity (the plateau), which evolves to lose completely the enzymatic activity at higher denaturant concentrations. Moreover, the Dm obtained by catalysis approaches better the Dm obtained in the secondary than in the tertiary unfolding transition. Thus, the enzymatic assays do confirm the above-proposed hypothesis: the existence of, at least, an intermediate state (I) in the unfolding process of the native xylanase (N) to the unfolded one (U). Therefore, the following scheme is proposed for the GdmCl unfolding of xylanase

$$N \leftrightarrow I \leftrightarrow U$$

The I state would show reduced activity and a secondary structure just like the native (Fig. 1b) but only part of its tertiary structure (Fig. 1c), showing a conformation lacking the compactness of the native state. We do not regard the possible effect on xylanase activity of GdmCl as a cation

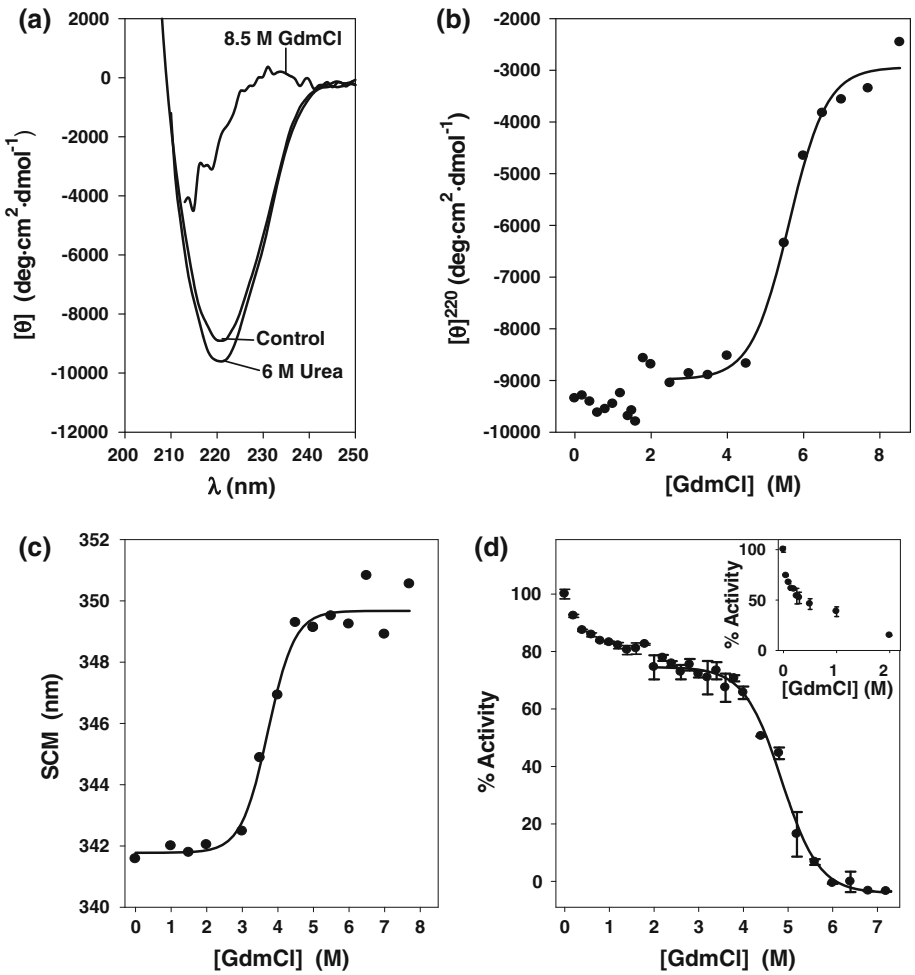


**Fig. 1** Far-UV circular dichroism, fluorescence intensity, and catalytic activity study of xylanase with GdmCl. **a** Mean residues ellipticities [$\theta$] vs. wavelength from the far UV-CD spectra of xylanase with 8.5 M GdmCl, 6 M urea and without denaturant in 20 mM citrate buffer pH 5. **b** Unfolding transition of xylanase by plotting the $[\theta]^{220}$ vs. GdmCl concentration. The *line* is a fit of data above 2 M to Eq. (2). **c** Variation of the spectral center of mass (SCM) with GdmCl concentration. The *line* is a fit of the data to Eq. (2). **d** Percent residual activity of xylanase vs. GdmCl concentration. Xylanase (1.4 μg) was preincubated with 0–7.3 M GdmCl in 100 μl of 100 mM citrate buffer pH 5 for 24 h at 4°C, then assayed for activity in standard condition (GdmCl become diluted 20 times in the assay). The *line* is the fit to Eq. (2) of data above 2 M GdmCl. *Inset* percent xylanase activity from enzymatic assays with the indicated GdmCl concentrations in the bulk reaction mixture

**Table 1** Thermodynamic data of xylanase unfolding by GdmCl and urea followed by tryptophan fluorescence and CD

| | GdmCl | | | Urea | | | | |
|---|---|---|---|---|---|---|---|---|
| | Dm (M) | $\Delta G^0_{H_2O}$ (kJ mol$^{-1}$) | $m$ (kJ mol$^{-1}$ M$^{-1}$) | Dm (M) | | | $\Delta G^0_{H_2O}$ (kJ mol$^{-1}$) | $m$ (kJ mol$^{-1}$ M$^{-1}$) |
| $[\theta]^{220}$ | 5.6 ± 0.1 (N–U) | 22.15 | 3.93 | 5.7 ± 0.2 (I–U) | | | 16.46 (I–U) | 3.49 |
| SCM | 3.7 ± 0.1 (N–U) | 17.22 (N–U) | 4.58 (N–U) | 2.7 ± 0.04 (I1–I2) | 6.7 ± 0.3 (I2–U) | | 16.65(I2–U) | 2.66(I2–U) |
| Activity | 4.9 ± 0.5 (I–U) | nd | nd | 1.1 ± 0.12 (N–I1) | 4.8 ± 0.3 (I1–I2) | 6.9 ± 0.4 (I2–U) | nd | nd |

Dm is the denaturant concentration at the midpoint transition in SCM or activity dependence on denaturant. The $m$ values are the slopes of fitting data from Fig. 1b (N ↔ U transition) Fig. 1c (N ↔ U transition) Fig. 2b (I2 ↔ U transition) and Fig. 2c (I ↔ U transition) to Eq. (4) and the $\Delta G^0_{H_2O}$ apparent values are the intercepts obtained by LEM in the respective transitions

*nd* Not determined

(on the catalytic acid residues since the protein is itself a cation at pH 5) in addition to its role as denaturant at low concentration, as suggested for other xylanases [22]. The reason for this exclusion is that xylanase activity is not sensitive to increasing ionic strength up to 1 M NaCl (not shown) and that the actual GdmCl concentration in enzymatic assay is 20 times smaller than in the preincubation medium due to substrate and buffer dilution. Therefore, the actual GdmCl concentration in the plateau of Fig. 1d is 0.1–0.2 M and thus, ionic strength remains low in the enzymatic assay. Therefore, the only effect of GdmCl on xylanase is as chaotropic agent. On the other hand, as GdmCl of the preincubation sample remains in the enzymatic assays although very diluted, we could doubt if results in Fig. 1d

were due to the effect of the residual GdmCl on xylanase activity instead of (or in addition to) the former effect of GdmCl on xylanase in preincubation samples. To clear this point, we measured the catalytic activity of xylanase with GdmCl but lacking preincubation with it. Results were plotted in Fig. 1d (inset) and showed a different shape than that obtained after preincubating xylanase with the chaotrope. For example, at 0.36 M GdmCl in inset, xylanase shows about 50% residual activity whereas at the same actual concentration (0.36 M) in the assay in Fig. 1d (7.2 M in the preincubation and in the figure) the activity is completely lost. Thus, the effect of GdmCl on xylanase depicted in Fig. 1d may be attributable to the changes that GdmCl produces in the enzyme during the preincubation period.

## Unfolding of xylanase by urea

The unfolding of xylanase induced by increasing concentrations of urea (0–8.6 M) monitored by far-UV CD, intrinsic fluorescence spectroscopy and catalytic activity are shown Fig. 2. Figure 2a depicts the xylanase intrinsic fluorescence spectra without denaturant and in the presence of increasing urea concentrations. We see that the fluorescence intensity (FI) decreases with urea to increase with further urea concentration thereafter. Figure 2b shows the variation of the SCM with urea concentration and a sharp decrease is noted from 0 M (N state) to 0.5 M urea, becoming stabilized up to 2.5 M (I1 state) and increasing thereafter to reach a plateau (3–4.5 M, I2 state) followed by a cooperative transition to the unfolded form (U). The unfolding process regarding the tertiary structure is described by:

$$N \leftrightarrow I1 \leftrightarrow I2 \leftrightarrow U$$

The fitting of the data to Eq. (2) gives the midpoint values for the transitions summarized in Table 1: $Dm = 2.7 \pm 0.04$ M (I1 $\leftrightarrow$ I2 transition) and $Dm = 6.7 \pm 0.3$ M (I2 $\leftrightarrow$ U transition). The plot of the $[\theta]^{220}$ vs. urea concentration is plotted in Fig. 2c. The N state in absence of urea was converted to an intermediate state (I) with $[\theta]^{220}$ more negative, thus stabilized ($\sim$44% $\beta$-sheet) and converted to the U form cooperatively. We must take into account that

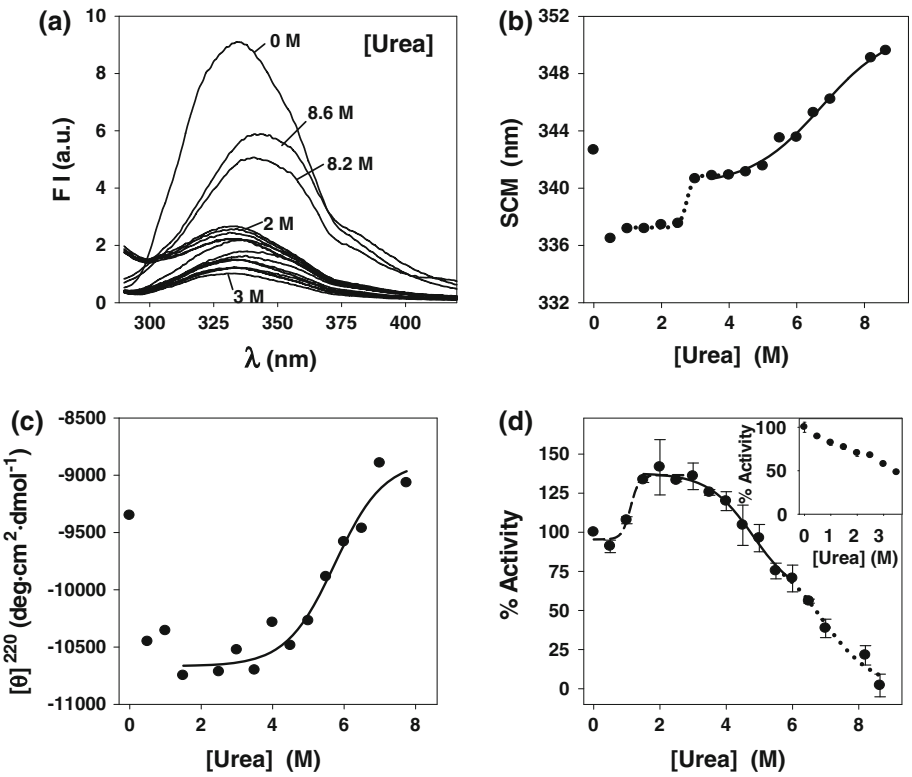


**Fig. 2** Far-UV circular dichroism, fluorescence intensity, and catalytic activity study of xylanase with urea. **a** Fluorescence intensity spectra of xylanase recorded with 0–8.6 M urea in 20 mM citrate buffer pH 5. **b** Unfolding transition of xylanase through the variation of SCM with urea concentration. The *line* is the fit to Eq. (2) of data above 2 M urea. **c** Unfolding transition of xylanase trough the variation of $[\theta]^{220}$ vs. urea concentration. The *line* is a fit of data above 1.5 M to Eq. (2). **d** Percent residual activity of xylanase vs. urea concentration. Xylanase (1.4 μg) was preincubated with 0–8.6 M urea in 100 μl of 100 mM citrate buffer pH 5 for 24 h at 4°C, then assayed for activity in standard condition (urea become diluted 20 times in the assay). There are three lines from fitting partial data to Eq. (2): 0–3 M urea (*dashed line*), 1.5–6 M (*solid line*), and 5.5–8.6 M (*dotted line*). *Inset* percent xylanase activity from enzymatic assays with the indicated urea concentrations in the bulk reaction mixture

xylanase with 6 M urea shows a molar ellipticity more negative than control (Fig. 2c and the spectrum of xylanase with 6 M urea in Fig. 1a), which seems to indicate that the only intermediate state seen in the ellipticity profile, still holds at this high denaturant concentration. Moreover, the changes occurring in the tertiary structure of xylanase (two intermediate states) are not reflected in its backbone.

The stability of xylanase against urea was also studied by monitoring the changes in enzymatic activity at increasing denaturant concentrations. Preincubation with the denaturant and enzymatic assays were carried out as described above for GdmCl. The residual activity vs. urea concentration (0–8.6 M) is depicted in Fig. 2d, where we see that there is an enhancement of the activity (maximum of ~40%) at low urea concentrations (1.5–3 M) followed by a gradual decrease in activity up to total loss at higher urea concentrations. However, this decrease does not appear cooperative and can be break down into two transitions with a mini-plateau at 5–5.5 M urea, which allowed a better fitting of the data. The unfolding process would depart with the N state, which at medium urea concentration (1.5–3 M) would give an intermediate state (I1) with enhanced activity (in parallel to the SCM drop in Fig. 2b). Then, as urea is further increased, the conformer I1 unfolds partially to give a second intermediate (I2) at 5–5.5 M urea which, in turn, totally unfolds to produce the U form of the enzyme. From the overall observation of SCM and catalytic changes with urea, we suggest the following pattern for the equilibrium denaturation of urea:

$$N \leftrightarrow I1 \leftrightarrow I2 \leftrightarrow U$$

Multi-state transitions are generally modeled as the superposition of independent two-state processes [14], thus the midpoint for the three transitions was obtained by fitting the data to Eq. (2) and is summarized in Table 1. Dm = 1.1 ± 0.1 M for urea activation (N ↔ I1 transition) and Dm = 4.8 ± 0.3 M and Dm = 6.9 ± 0.4 M for I1 ↔ I2 and I2 ↔ U transitions, respectively.

## Thermodynamical stability of xylanase

Refolding of fully unfolded samples was achieved by diluting 50 times the denaturant (GdmCl or urea) with 0.1 M citrate buffer pH 5 and preincubating the samples for 24 h at 4°C. Xylanase was refolded after urea dilution since 100% enzymatic activity was recovered whereas ~60% activity was recovered after GdmCl dilution. As xylanase unfolding can be seen as a reversible process, thermodynamic treatment of the data can be applied to our results. The conformational stability of a protein that undergoes a reversible transition is given by its $\Delta G^0_{H_2O}$ [30]. $\Delta G^0_{H_2O}$ is calculated from the free energy ($\Delta G^0$) vs. denaturant concentration plot. The free energy in the GdmCl and urea unfolding, was obtained applying Eq. (3) to data represented in Fig. 1b (N ↔ U transition), Fig. 1c (N ↔ U transition), and Fig. 2b (I2 ↔ U transition). Thus, chemical unfolding curves at different denaturants concentrations were analyzed using a two-state unfolding mechanism, according to the linear extrapolation model (LEM) [38]. Figure 3 depicts plots of the linear dependence of free energy variation with GdmCl (Fig. 3a) or urea (Fig. 3b) concentration in the SCM dependence of denaturant. We see that at low denaturant concentration, the native state is favored and $\Delta G^0 > 0$ whereas at high denaturant concentrations, $\Delta G^0 < 0$, so that unfolding is favored. At some denaturant concentration, both the native and denatured states will be equally favored and $\Delta G^0 = 0$. The fitting of the data in Fig. 3a and b to Eq. (4) and data from Fig. 1b (not shown) allowed to calculate the free energy in water, at zero denaturant concentration ($\Delta G^0_{H_2O}$, the intercept) and m (the slope). Results are summarized in Table 1. $\Delta G^0_{H_2O}$ represents the difference in free energy between the native and the denatured state of the protein extrapolated to 0 M denaturant and is $\Delta G^0_{H_2O} = 17.22$ kJ mol$^{-1}$ and $\Delta G^0_{H_2O} = 16.65$ kJ mol$^{-1}$ M$^{-1}$ for GdmCl and urea unfolding curves, respectively (SCM transition), which gives a mean value of $\Delta G^0_{H_2O} \sim 16.9$ kJ mol$^{-1}$. The values obtained for GdmCl and urea in the molar ellipticity transition were $\Delta G^0_{H_2O} = 22.15$ kJ mol$^{-1}$ and 16.46 kJ mol$^{-1}$, respectively, (not shown as figures, summarized in Table 1). Regarding the *m* value (the slope), it is an empirical parameter reflecting the change in solvent exposure of the protein during the transition, and therefore, it is considered an index of the compactness of the protein or a measure of the cooperativity of the denaturation [31]. The values $m = 4.58$ kJ mol$^{-1}$ M$^{-1}$ for GdmCl and $m = 2.66$ kJ mol$^{-1}$ M$^{-1}$ for urea in the SCM unfolding transitions and $m = 3.93$ kJ mol$^{-1}$ M$^{-1}$ and $m = 3.49$ kJ mol$^{-1}$ M$^{-1}$ for GdmCl and urea transitions, respectively ($[\theta]^{220}$ measure), indicate that the changes occurring in the loops of the protein where Trp/s is/are located are more cooperative when xylanase is unfolded with GdmCl than with urea since *m* is higher and so occurs in the backbone unfolding transition. This was expected since at high urea concentration, the theoretically unfolded state of xylanase probably possesses some folded structure as seen for other proteins whereas proteins denatured by GdmCl closely approach a random coiled conformation [17], thus a lower m value was expected when xylanase was unfolded with urea.

## Effect of trifluoroethanol on xylanase conformation

Changes in the secondary structure of xylanase were followed by changes in $[\theta]^{220}$ (Fig. 4a) and SCM (Fig. 4b) with increasing % TFE (v/v) in the preincubated xylanase

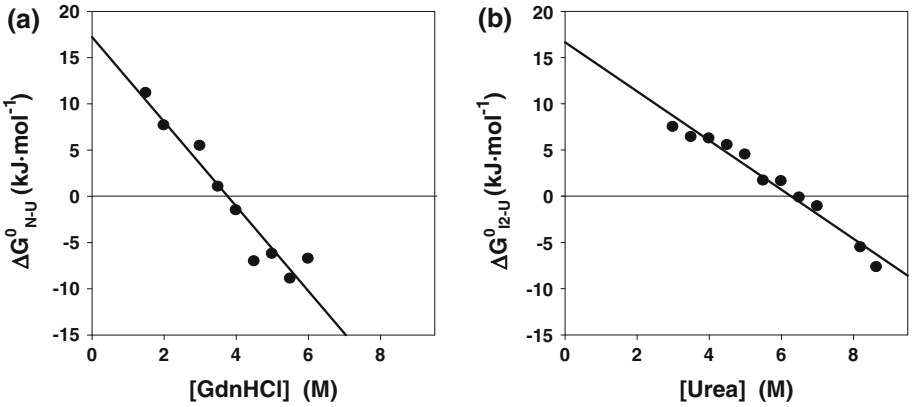


**Fig. 3** Variation of the Gibbs energy with GdmCl and urea concentrations. **a** Values of $\Delta G^0$ obtained by applying Eq. (3) to data of Fig. 1c (SCM) plotted vs. GdmCl concentration. The *line* in the plot is a fit of the data to Eq. (4) and is extended to the *Y*-axis. **b** Same as in **a** except that SCM data (from Fig. 2b of the urea unfolding process) were plotted vs. urea concentration

sample. As expected for TFE effect, the $[\theta]^{220}$ of xylanase became more negative in parallel with the increased in α-helix content and decrease in β-sheet (Fig. 4b) whereas the SCM increased in a cooperative mode (Fig. 4c). The fitting of data to Eq. (2) gave 62.7 ± 2% (Fig. 4a) and 30.9 ± 1.7% (Fig. 4c) as the midpoint TFE of the secondary and tertiary structure transitions, respectively, indicating that changes occurring in the trp residues environment occur at a lower TFE than those affecting the backbone of the enzyme. Enzymatic assays of xylanase preincubated with TFE for 24 h at 4°C were carried out and residual percent activity is depicted in Fig. 4d vs. TFE concentration. The midpoint transition 39.1 ± 1.7% (v/v) is the TFE necessary to half reduce xylanase activity. This value is far greater than that obtained when xylanase was assayed with the indicated TFE concentration (9.3 ± 0.5% (v/v), Fig. 4d, inset). As there is 20 times dilution of TFE in the assay when preincubation took place, the actual midpoint in the enzymatic assay would be about 2% TFE. A TFE value so low should maintain the enzyme fully active (as shown in the inset). Nevertheless, there is inactivation and therefore, the effect of TFE in Fig. 4d is on the enzyme conformation while xylanase was preincubated with it, thus, it is a stability effect.

## Effect on xylanase of pH changes

Stability of xylanase to pH changes was studied by spectroscopic techniques and catalytic activity and results are depicted in Fig. 5. The molar ellipticity at 220 nm does not

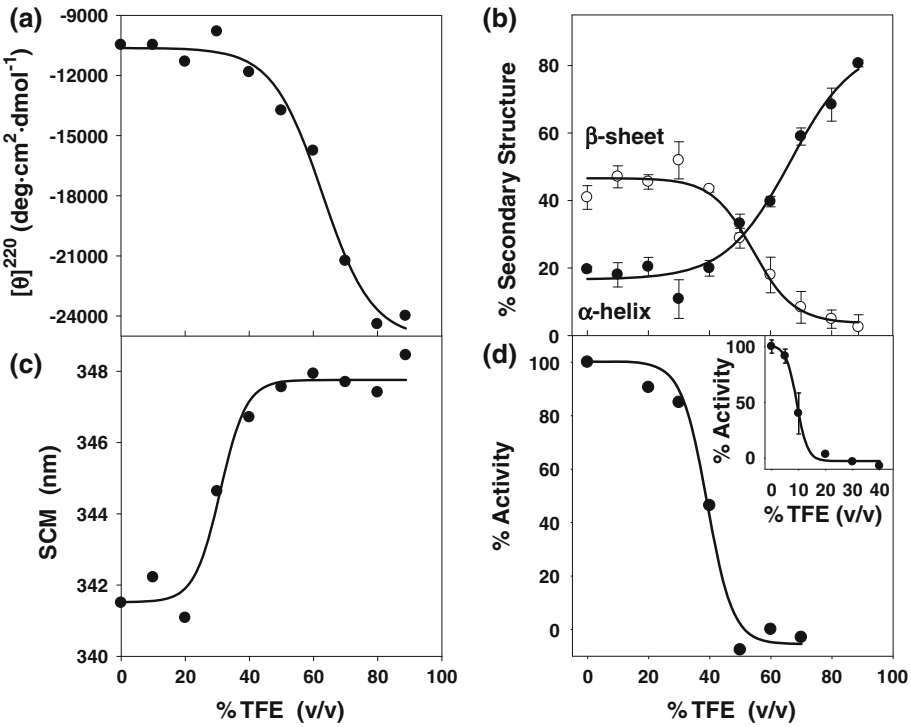


**Fig. 4** Effect of trifluoroethanol on xylanase secondary and tertiary structure and enzymatic activity. **a** Dependence of molar ellipticity at 220 nm on TFE concentration. **b** Variation of α-helix (*filled circles*) and β-sheet (*void circles*) with TFE concentration. **c** Dependence of SCM on TFE concentration. **d** Stability of xylanase to TFE. The enzyme (1.4 μg in 100 mM citrate buffer) was preincubated with the alcohol for 24 h at 4°C in 100 μl, then assayed for activity (TFE concentration in the assay become diluted 20 times). *Inset* Enzymatic assay of 1.4 μg xylanase in standard conditions except for the presence in the assay of the indicated TFE concentration. *Lines* in plots are fits to Eq. (2)

vary noteworthy with pH in the range 2–9 (Fig. 5a), indicating a great stability of the backbone of xylanase to changes in the protonation of their amino acid residues. Regarding the tertiary structure, we see in Fig. 5b that the SCM varies cooperatively upon acidification with a midpoint transition: pKa = 3.3 ± 0.3. This indicates that the protonation of an amino acid residue with this pKa triggers the conformational change. As SCM is increased, the tryptophan residues are displaced to an environment more polar in parallel to the displacement of the wavelength where the maximum fluorescence intensity occurs, from 335 to 337 nm (not shown). No relevant conformational change is observed in the alkaline pH range. Figure 5c plots the residual activity of xylanase after preincubating it in CMT buffer at pH 2.5–8.5 either for 30 min or 22 h at 25°C. The enzyme is stable from pH 3.5 to 8.5 when preincubated 30 min whereas it maintains 80% activity at pH 5.5–8.5 to decrease at acid pHs thereafter at the longer preincubation time (22 h). Our results are quite similar to previous reports of xylanase II from *Trichoderma reesei* Rut C-30 [42] and of recombinant xylanase expressed in *E. coli* although several mutants showed wider pH profiles at higher temperatures [45]. The profile of activity vs. pH depicted in Fig. 5d shows a typical shape with maximum activity at pH 5 and also agrees with previous reports [45] except that our profile is wider and shows 35% activity at pH 8 instead of losing the activity [42].

## Bis-ANS binding studies

The intermediates in the GdmCl and urea unfolding exhibited the characteristics of the molten globule state of proteins regarding secondary and tertiary structure [33].To asses the molten globule nature of the intermediate in the unfolding processes, we used a fluorescent probe that can neither bind the native nor the unfolded state of proteins but can bind intermediate structures with hydrophobic domains exposed to the medium [23]. Therefore, it is a sensitive probe to detect molten globule states of proteins, in which secondary structural elements are established, but the packing of the side chains in the hydrophobic core is not yet complete, giving rise to a fluctuating globular structure [4]. The effect that the environment of the xylanase has on the fluorescence emission of bis-ANS at 480 nm is shown in Fig. 6. Changes in the intensity of fluorescence emission by bis-ANS were observed as GdmCl and urea concentration were increased (Fig. 6a). In the presence of urea, there is a broad emission peak that

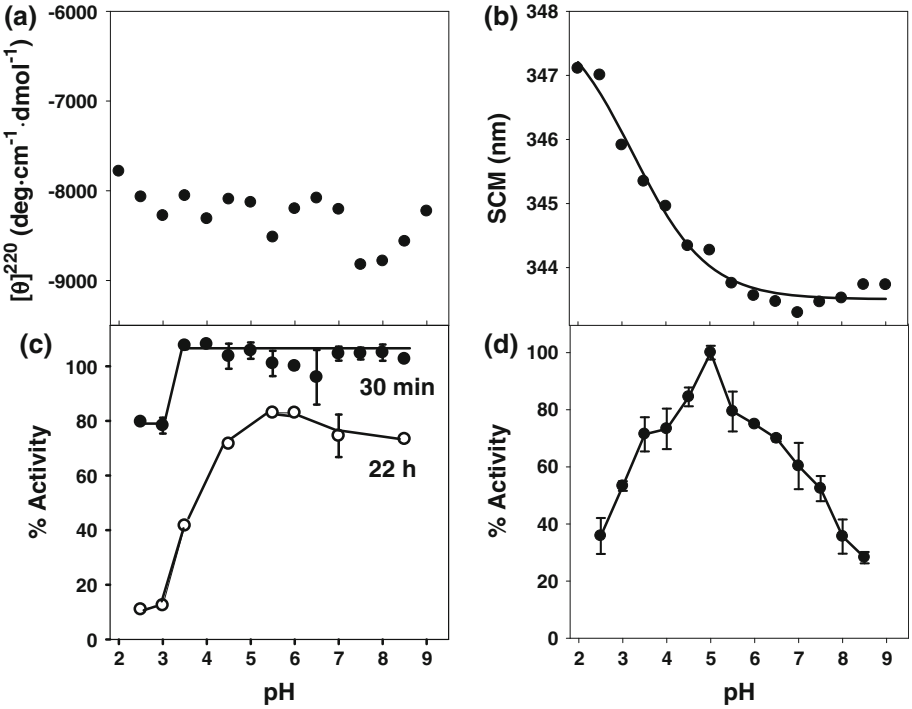


**Fig. 5** Far-UV CD and fluorescence spectroscopies of xylanase with pH changes. Stability and activity of xylanase with pH. **a** The molar ellipticity at 220 nm plotted vs. pH. **b** Dependence of SCM on pH changes. The *line* is a fit to Eq. (2) by changing *D* and Dm for pH and pKa. **c** Stability of xylanase to pH. Protein (1.4 μg) was preincubated in 200 μl of CMT buffer (5 mM) at the indicated pH for 30 min or 22 h at 25°C. Samples were assayed for activity in 2 ml of final volume of 100 mM citrate buffer pH 5 containing 1% xylan. Other conditions are as described in "Materials and methods". Results are expressed as residual percent activity taking 100% the activity of the enzyme not preincubated. **d** Activity of xylanase with pH. Protein (1.4 μg) was assayed for activity in 2 ml of CMT buffer (5 mM) at the indicated pH containing 1% xylan. Other conditions are as described in **c**, except that 100% was the activity at pH 5

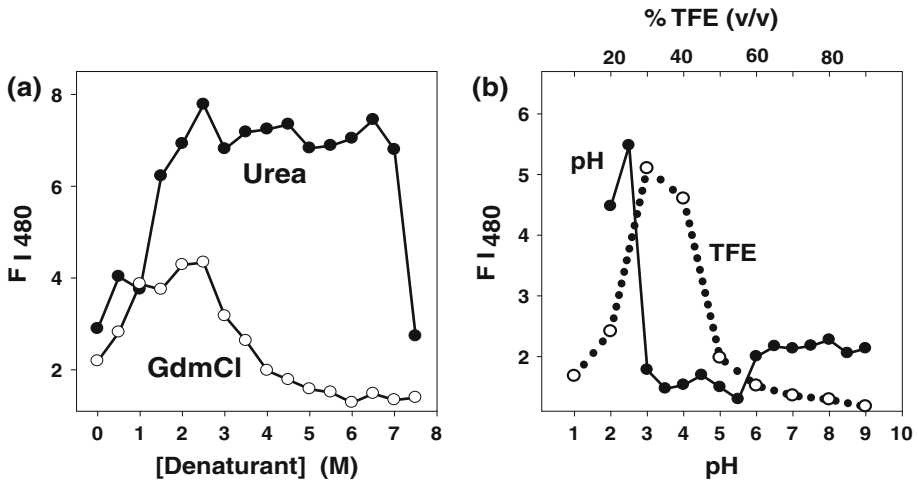


**Fig. 6** Fluorescence intensity emitted by bis-ANS with xylanase and denaturants, TFE, and pH changes. **a** Fluorescence intensity at 480 nm of the probe (8 μM) in the presence of xylanase (0.09 mg $ml^{-1}$) with GdmCl (*void circles*) or urea (*filled circles*) vs. the denaturant concentration in 20 mM citrate buffer pH 5. The spectra were recorded upon excitation at 395 nm. **b** Same as in **a** except that xylanase samples do not contain chaotropes and were in CMT buffer at the indicated pH (*filled circles*, *solid line*) or were in 20 mM citrate buffer pH 5 and contained TFE at the indicated concentration (*void circles*, *dotted line*)

may correspond to the emission of the probe bound to the intermediate states, I1 and I2, detected and commented in Fig. 2. We must remark that at 6 M urea, the probe still shows emission, which is in agreement with data from Figs. 2c and 1a commented above, pointing to the intermediate state still existing at so high denaturant concentration. Only at 7.5 M urea, the fluorescence intensity reaches the control value in absence of urea indicating that xylanase has been unfolded. When xylanase is in the presence of GdmCl, the probe also shows fluorescence emission, although the peak is narrower than that shown with urea. This result is also concordant with the existence of one intermediate state, I, in the catalytic stability study in Fig. 2d. There is also a coincidence between the GdmCl concentration at the maximum emission (2–2.5 M) and at the plateau in Fig. 2d, where an intermediate with reduced residual activity (~70%) was observed. With both denaturants the existence of intermediate states with molten globule structure is confirmed although the fact that the emission is greater with urea than with GdmCl could point to xylanase intermediate states exhibiting a higher number of hydrophobic residues where the probe can bind when the unfolding chemical was urea. Figure 6b plots the FI at 480 nm of bis-ANS emission in the presence of xylanase at different pHs. A noteworthy fluorescence emission of the probe is noted at pH 2 and 2.5, thus characterizing molten globule structures only at the indicated pH. Also, the probe emits when xylanase is in a medium with 30–40% TFE (v/v), which is just the TFE concentration in the SCM transition between the folded and unfolded form of the enzyme in Fig. 4b. Therefore, xylanase shows molten globule structures also at very low pH and 30–40% TFE.

## Discussion

Protein folding is a highly cooperative process, which, for small globular proteins may be approximate by a two-state process although proteins with more than 100 amino acid residues fold usually in more than two-state process [34]. Denaturation studies can yield information about the native state in terms of its cooperativity, intrinsic stability, and the nature of forces required to maintain the tertiary structure. In order to gain information about the conformational stability of xylanase II from *T. reesei* QM 9414, we proceeded to perform the classical approach of unfolding the protein in presence of GdmCl and urea as well as other environment perturbing agents such TFE and pH changes by means of CD, intrinsic and extrinsic fluorescence spectroscopy, and enzymatic assays. Xylanase unfolds in a three-state process in the presence of GdmCl being the intermediate state detected through enzymatic stability assays (~70% residual activity, 2–4 M GdmCl) but not with the conformational studies where two-state transitions were observed and finally confirmed by the binding of bis-ANS. Changes in xylanase tertiary structure are displayed at lower GdmCl concentration ($Dm = 3.7 \pm 0.1$ M) than changes in its secondary structure ($Dm = 5.6 \pm 0.1$ M). At 5.5 M GdmCl, the enzyme shows practically no activity and the tertiary structure is almost lost but still conserves part of its secondary structure (see Fig. 1). This is not surprising since it has been shown that inactivation of other enzymes precedes conformational changes during denaturation by GdmCl, suggesting that the enzyme active sites are located in regions more susceptible to perturbation by denaturants than the molecule as a whole. Thus, it may occur that the conformation of the active site is held

together by weaker forces than the overall structure [51]. Unfolding of xylanase by urea is, at least, a four-state process as suggested by results in Fig. 2 where two intermediate states (at ~2 and ~4 M urea) are seen clearly in the SCM dependence of urea concentration whereas only one is detected regarding the backbone of the protein (at 2–4 M urea, Fig. 2c).Regarding the enzymatic stability of xylanase with urea, one of the intermediate states displays ~40% enhanced activity and the other ~70% residual activity. The midpoints of these transitions are summarized in Table 1. The activating effect of urea on enzymatic activity has been previously reported in *Chainia* xylanase either at slight acid or alkaline pH [22]. The intermediate states of xylanase chemical unfolding exhibit the characteristics of molten globule structures, that is, conserved secondary structure, partial lost of tertiary structure and binding to the fluorescent probe bis-ANS.

The reversibility of the unfolding process with both denaturants allowed the thermodynamic treatment of the data. The conformational stability of xylanase, the difference in Gibbs energy between the folded and the unfolded states, has been determined using the LEM. The extrapolated value $\Delta G^0_{H_2O}$ (in absence of denaturants) is practically identical for both GdmCl and urea in the tertiary structure unfolding process, that is, 17.22 kJ $mol^{-1}$ and 16.65 kJ $mol^{-1}$, respectively, and slightly higher: 22.15 kJ $mol^{-1}$ for the backbone unfolding process with GdmCl but again identical 16.46 kJ $mol^{-1}$. The mean $\Delta G^0_{H_2O}$ is in the low range of values reported for globular proteins where the native state appears to be stabilized by 17.7–83.6 kJ $mol^{-1}$ [40] or 21–41.8 kJ $mol^{-1}$ [31]. As the native conformation of most globular proteins is only marginally more stable (~20–60 kJ $mol^{-1}$) than a randomly coiled conformation under physiological conditions [41], the values we found for the Gibbs energy of xylanase are not surprising. The reason for this is that enzymes need plasticity and rapid changes in conformation to accommodate substrates and to catalyze, and a low thermodynamic stability favors these functions. One of the suggested strategies that evolution may have developed in order to keep large proteins from becoming too stable is the increased number of buried charged groups they display [20].

The effect of TFE on xylanase conformation and enzymatic stability was also studied since TFE is known to promote changes in the secondary structure of proteins. The addition of TFE to protein samples must decrease the polarity of the solvent promoting peptide hydrogen bonds, thus α-helix formation, while discouraging hydrophobic interactions [50]. Because hydrophobic interactions are important for the stabilization of β-sheet structures, a parallel decrease in β-sheet content of xylanase with an increase in TFE concentration was expected. Results of xylanase α-helix and β-sheet content with increasing TFE follows the expected pattern of α-helix increase and concomitant β-sheet decrease. However, TFE is not a helix-inducing solvent in the sense that it will induce helix formation independently of the sequence. It is rather a helix-enhancing cosolvent, which stabilizes helices in regions with some α-helical propensity. A model has been developed to explain the effect of TFE on the secondary structure of proteins and peptides. At low alcohol concentrations (0–10% v/v), where the TFE clusters are not fully developed or stabilized, TFE draws water away from the surface of proteins. As the TFE concentration increases and the cluster size becomes larger, the clusters may associate directly with the hydrophobic side chains. This decreases the side-chain conformational entropy, which may be important in the formation of α-helix structures [35]. In parallel to secondary structure changes in xylanase with increasing TFE, tertiary structure and enzymatic stability were also affected. This result was expected since family 11 xylanases present one single (catalytic) domain with an all-β-strand "sandwich-like" fold containing two β-sheets forming a large cleft that can accommodate the xylan polymers. On either side of the open cleft are two conserved glutamate residues which have been identified as the nucleophilic and acid/base catalysts [44]. Thus, if β-sheet content diminishes with TFE increase, in addition to changes in the tertiary structure, xylanase could not hold a catalytic pocket designed precisely to be in between β-sheets.

Finally, to complete the stability study, the pH changes were considered as possible protein conformers makers. Nevertheless, we found that the secondary structure and the enzymatic activity are rather stable to pH changes whereas the tertiary structure begins to unfold as the pH is acidified below 4, although in the alkaline side, the tertiary structure remains unchanged. In general, xylanases that are stable in alkaline conditions are typically characterized by having a decreased number of acidic residues and an increased number of arginines [46] whereas tertiary structure analysis of family 11 xylanases from *T. reesei* indicated that adaptation to low pH is brought about by an increase in negative charge and a substitution and reorientation of aromatic residues in the active sites [44]. In this aspect, xylanase from *T. reesei,* although an alkaline enzyme, shows a moderate balance (ten basic residues vs. eight acid residues, DNA star program) which would explain the quasi flat profiles of secondary structure and enzyme stability with varying pH and the modest loss of tertiary structures at very acid pH (2.5) with the concomitant formation of a molten globule structure. To complete the studies on xylanase stability, work is now in progress to find the conformational basis of its thermal stability with a point in employing differential scanning calorimetry to

contrast the thermodynamic stability of xylanase (this paper) with new calorimetric data.

**Acknowledgments** Research in the laboratory of the authors was funded by grants from Spanish Ministry of Science (BIO2009-09694).

## References


1. Acebal C, Castillón MP, Estrada P, Mata I, Costa E, Aguado J, Romero D, Jiménez F (1986) Enhanced cellulase production from *Trichoderma reesei* QM 9414 on physically treated wheat straw. Appl Microbiol Biotechnol 24:218–223
2. Anbarasan S, Janis J, Poleheimo M, Laitaoja M, Vuolanto M, Karimaki J, Viniotalo P, Leisola M, Turunen O (2010) Effect of glycosylation and additional domains on the thermostability of a family 10 xylanase produced by *Thermopolyspora flexuosa*. Appl Environ Microbiol 76:356–360
3. Biely P (1985) Microbial xylanolytic system. Trends Biotechnol 3:286–290
4. Chapeaurouge A, Johansson JS, Ferreira ST (2002) Folding of a de novo designed native-like four-helix bundle protein. J Biol Chem 10:16478–16483
5. Ciechanska D (2003) Progress in biomodification of cellulose pulps by cellulases and xylanases. Fibres textiles East Eur 3:74–78
6. Cobos A, Estrada P (2003) Effect of polyhydroxylic cosolvents on the thermostability and activity of xylanase from *Trichoderma reesei* QM 9414. Enzyme Microb Technol 33:810–818
7. Collins T, Meuwis MA, Gerday C, Feller G (2003) Activity, stability and flexibility in glycosidases adapted to extreme thermal environments. J Mol Biol 328:419–428
8. Dawoodi J, Wakarchuk WW, Carey PR, Surewicz WK (2007) Mechanism of stabilization of *Bacillus circulans* xylanase upon the introduction of disulfide bonds. Biophys Chem 125:453–461
9. Dueñas MJ, Estrada P (1996) Immobilization of $\beta$-xylosidase from *Trichoderma reesei* QM 9414 on nylon powder. Biocatal Biotrans 17:139–161
10. Dutta T, Bhattacharjee A, Majumdar U, Ray SS, Sahoo R, Ghosh S (2009) In vitro renaturation of alkaline family G/11 xylanase via a folding intermediate: $\alpha$-crystallin facilitates refolding in an ATP-independent manner. Appl Biochem Biotechnol. doi: 10.1007/s12010-009-8854-y
11. Estrada P, Mata I, Domínguez JM, Castillón MP, Acebal C (1990) Kinetic mechanism of ∃-glucosidase from *Trichoderma reesei* QM 9414. Biochim Biophys Acta 1033:298–304
12. Fan YX, McPhie P, Miles EW (1999) Guanidine hydrochloride exerts dual effects on the tryptophan synthase $\alpha 2\beta 2$ complex as a cation activator and as a modulator of the active site conformation. Biochemistry 38:7881–7889
13. Fukumura M, Tanaka A, Sakka K, Ohmiya K (1995) Process of thermal denaturation of xylanase (XynB) from *Clostridium stercorarium* F-9. Biosci Biotech Biochem 59:47–50
14. Godzek A, Stankiewicz-Drogon A, Poznanski J, Boguszewska-Chachulska AM (2008) Circular dichroism analysis for multidomain proteins: studies of the irreversible unfolding of *Hepatitis C virus* helicase. Acta Biochem Polonica 55:57–66
15. Gómez M, Isorna P, Rojo M, Estrada P (2001) Kinetic mechanism of $\beta$-xylosidase from *Trichoderma reesei* QM 9414. J Mol Cat B Enzym 16:7–15
16. Gómez M, Isorna P, Rojo M, Estrada P (2001) Chemical mechanism of $\beta$-xylosidase from *Trichoderma reesei* QM 9414: pH-dependence of kinetic parameters. Biochimie 83:961–967
17. Greene RF Jr, Pace CN (1974) Urea and guanidine hydrochloride denaturation of ribonuclease, lysozyme, $\alpha$-chymotrypsin and $\beta$-lactoglobulin. J Biol Chem 17:5388–5393
18. http://www.us.expasy.org/cgi-bin/protparam
19. Jänis J, Rouvinen J, Leisola M, Turunen O, Vainiolato P (2001) Thermostability of endo-1,4-$\beta$-xylanase II from *Trichoderma reesei* studied by electrospray ionization Fourier-transform ion cyclotron resonance MS, hydrogen/deuterium-exchange reactions and dynamic light scattering. Biochem J 356:453–460
20. Kajander T, Kahn PC, Passila SH, Cohen DC, Lehtio L, Adolfsen W, Warwicker J, Shell U, Goldman A (2000) Buried charged surface in proteins. Struct Fold Des 8:1203–1214
21. Kaneko S, Ito S, Fujimoto Z, Kuno A, Ichinose H, Iwamatsu S, Hasegawa T (2009) Importance of interactions of the $\alpha$-helices in the catalytic domain N- and C-terminals of the family 10 xylanase from *Streptomyces olivaceoviridis* E-86 to the stability of the enzyme. J Appl Glycosci 56:165–171
22. Kumar AR, Hedge SS, Ganeh KN, Khan MI (2003) Structural changes enhance the activity of *Chainia* xylanase in low urea concentrations. Biochim Biophys Acta 1645:164–171
23. Lima MR, Zingali RB, Foguel D, Monteiro RQ (2004) New insights into conformational and functional stability of human $\alpha$-thrombin probed by high hydrostatic pressure. Eur J Biochem 271:3580–3587
24. Lowry OH, Rosebrough NJ, Farr AL, Randall RT (1951) Protein measurement with the Folin phenol reagent. J Biol Chem 193:266–275
25. Maat J, Roza M, Verbakel J, Stam H, Santos da Silva MJ, Bosse M (1992) Xylanases and their application in bakery. In: Visser J, Beldman G, Kusters van Someren MA, Voragen AGJ (eds) Xylans and xylanases. Elsevier, Amsterdam, pp 371–378
26. Mata I, Domínguez JM, Macarrón R, Castillón MP, Estrada P (1990) Xylanase and $\beta$-xylosidase isolation from cultures of *Trichoderma reesei* QM 9414. In: Grassi G (ed) Biomass for energy and industry. Elsevier, Amsterdam, pp 2283–2287
27. Miller GL (1959) Use of dinitrosalicylic acid reagent for determination of reducing sugars. Anal Chem 31:426–428
28. Nath D, Rao M (2001) Artificial chaperone mediated refolding of xylanase from a alkalophilic thermophilic *Bacillus* sp. (NCIM 59). Implications for in vitro protein renaturation via a folding intermediate. Eur J Biochem 268:5471–5478
29. Nath D, Rao M (2001) pH dependent conformational and structural changes of xylanase from an alkalophilic thermophilic *Bacillus* sp. (NCIM 59). Enzyme Microb Technol 28:397–403
30. Pace CN (1990) Measuring and increasing protein stability. Trends Biotechnol 8:93–98
31. Pappa HS, Cass AEG (1993) A step towards understanding the folding mechanism of horseradish peroxidase. Tryptophan fluorescence and circular dichroism equilibrium studies. Eur J Biochem 212:227–235
32. Parkinnen T, Hakulinen N, Tenkanen M, Siika-aho M, Rouvinen J (2004) Crystallization and preliminary X-ray of a novel *Trichoderma reesei* xylanase IV belonging to glycoside hydrolase family 5. Acta Cryst 60:542–544
33. Ptitsyn OB (1996) Molten globule and protein folding. Adv Prot Chem 47:83–229
34. Radford SE (2000) Protein folding: progress made and promises ahead. Trends Biochem Sci 25:611–618
35. Reiersen H, Rees AR (2000) Trifluoroethanol may form a solvent matrix for assisted hydrophobic interactions between peptide side chains. Prot Eng 13:739–743
36. Roberge M, Shareck F, Morosoli R, Kluepfel D, Dupont C (1997) Characterization of two important histidine residues in the active site of xylanase A from *Streptomyces lividans,* a family 10 glycanase. Biochemistry 36:7769–7775

37. Robinson PD (1984) Cellulase and xylanase production by *Trichoderma reese*i Rut C-30. Biotechnol Lett 6:119–122
38. Santoro MM, Bolen DW (1988) Unfolding free energy changes determined by the linear extrapolation method. 1 Unfolding of phenylmethanesulphonyl alpha-chymotrypsin using different denaturants. Biochemistry 27:8063–8068
39. Sreerama N, Woody RW (2000) Estimation of protein secondary structure from circular dichroism spectra: comparison of CONTIN, SELCON, and CDSSTR methods with an expanded reference set. Anal Biochem 287:252–260
40. Tanford C (1964) Isothermal unfolding of globular proteins in aqueous urea solutions. J Am Chem Soc 86:2050–5059
41. Tanford C (1970) Protein denaturation C. Theoretical models for the mechanism of denaturation. Adv Protein Chem 24:1–95
42. Tenkanen M, Puls J, Pontanen K (1992) Two major xylanases of *Trichoderma reesei*. Enzyme Microb Technol 14:566–574
43. Törrönen A, Mach RL, Messner R, González R, Nisse K, Harkki A, Kubiceck CP (1992) Two major xylanases from *Trichoderma reesei:* characterization of both enzymes and genes. Biotechnol 10:1461–1465
44. Törronen A, Harkki A, Rouvinen J (1994) Three dimensional structure of endo $\beta$-1,4-xylanase II from *Trichoderma reesei*.: two conformational states in the active site. EMBO J 13:2493–2501
45. Turunen O, Etuaho K, Fenel F, Vehmaanpera J, Wu X, Rouvinen J (2001) A combination of weakly stabilizing mutations with a disulphide bridge in the $\alpha$-helix region of *Trichoderma reesei* endo-1,4-$\beta$-xylanase increases the thermal stability through synergism. J Biotechnol 88:37–46
46. Turunen O, Vourio M, Fenel F, Leisola M (2002) Engineering of multiple arginines into the Ser/Thr surface of *Trichoderma reesei* endo-$\beta$-1,4-xylanase II increases the thermo tolerance and shifts the pH optimum towards alkaline pH. Prot Eng 15:15–141
47. Viikari L, Kantelinen A, Sundquist J, Linko M (1994) Xylanases in bleaching: from an idea to industry. FEMS Microbiol Rev 13:335–350
48. Wassenberg D, Schurig H, Liebl W, Jaenicke R (1997) Xylanase XynA from the hyperthermophilic bacterium *Thermotoga maritima*: structure and stability of the recombinant enzyme and its isolated cellulose-binding domain. Protein Sci 6:1718–1726
49. Xu J, Takakuwa N, Nogawa M, Okada H, Morikawa Y (1998) A third xylanase from *Trichoderma reesei* PC-3–7. Appl Microbiol Biotechnol 49:718–724
50. Yamaguchi K, Naiki H, Goto Y (2006) Mechanism by which the amyloid-like fibrils of a $\beta$2-microglobulin fragment are induced by fluorine-substituted alcohols. J Mol Biol 363:279–288
51. Zhou HM, Zhang XH, Yin Y, Tsou CL (1993) Conformational changes at the active site of creatine kinase at low concentration of guanidinium hydrochloride. Biochem J 291:103–107